Correspondence

Quantitative Analysis of Ultrasound Contrast Agent Postexcitation Collapse

Daniel A. King and William D. O'Brien Jr.

***Abstract*—An empirically based peak-detection technique is described for statistically analyzing single ultrasound contrast agent collapses. It is shown that microbubbles with postexcitation collapse initially exhibit a stronger principal response on average than those without postexcitation, and that lower insonifying frequencies lead to postexcitation signals which have greater separation from their principal response and persist through more rebounds.**

I. Introduction

Ultrasound contrast agents (UCA) are gas-filled, encapsulated microbubbles typically on the order of 1 to 10 μm in diameter. UCAs undergoing nonlinear oscillations and destruction have been used for a variety of diagnostic and functional medical applications [1]–[5]. Therefore, experimental analysis of the dynamic response of UCAs to large amplitude forcing is an important intermediate step for both proper modeling of shelled microbubbles and also understanding the physical mechanisms which generate bioeffects. In this work, the rebound characteristics from a population of collapsing single UCAs are quantified through peak detection of the time-domain signal.

Double passive cavitation detection (PCD) has demonstrated utility as an acoustic characterization technique with the ability to distinguish responses among different commercially available UCAs [6]. The observed postexcitation rebound, which is indicative of shell rupture, inertial cavitation, and destruction of the UCA, has also been shown to fit with predictions of the Marmottant shelled bubble model [7], [8]. This study builds upon prior experimental work by quantifying the distinctions between postexcitation and non-postexcitation responses as well as frequency-dependent effects on postexcitation. Although previous results successfully used manual classification from multiple individuals, the process of visual inspection was both susceptible to varied qualitative interpretations and time consuming; this limited the amount of data that could be reasonably analyzed in a study. Therefore, an automatic classification routine based on peak detection parameters was developed to imitate ideal manual classification guidelines and to standardize data analysis across acoustic parameters.

Manuscript received April 1, 2014; accepted April 25, 2014. This research was supported by the National Institutes of Health under grant number R37EB002641.

D. A. King is with the Department of Mathematical Sciences, Eastern Mennonite University, Harrisonburg, VA (e-mail: daniel.king@emu.edu).

W. D. O'Brien Jr. is with the Department of Electrical and Computer Engineering, University of Illinois at Urbana-Champaign, Urbana, IL.

DOI http://dx.doi.org/10.1109/TUFFC.2014.3023

II. Materials and Methods

The double PCD technique involved confocal alignment of two higher frequency passive receive transducers placed at a 90° angle with one lower frequency active transmit transducer placed equally between them at a 45° angle. The Valpey-Fisher transducers (CTS Valpey Corp., Hopkinton, MA) were characterized and calibrated according to established procedures (Table I) [9]–[11]. A very low concentration of approximately 5000 UCAs/mL of Definity (Lantheus Medical Imaging, Inc., North Billerica, MA) was introduced into the tank containing degassed, room-temperature water, and short-duration (3-cycle), large-amplitude pulses [1 to 7 MPa peak rarefactional pressure amplitude (PRPA)] were used to insonify the gently stirred UCAs.

Upon data acquisition, the signals from the two high-frequency receive transducers were processed to classify the UCA behavior based on the acoustic response. Two general features in the time domain were of interest—the principal response (PR), which was the forced response of the UCA to the transmit pulse, and the postexcitation signal (PES), which was a broadband spike following and separated in time from the PR [Fig. 1(a)].

The automatic classification routine to identify the categories was comprised of a multistep process. First, a relatively large noise threshold, ξ, was identified before the injection of UCAs as 3.3 standard deviations from the mean of the Gaussian noise; this was on the order of a few millivolts in this specific experimental setup and was used to define clearly observable UCA responses. The period, T, associated with the transmit center frequency was used for a frequency-independent time metric. Because of the large-amplitude pulses, the forced UCA oscillations were primarily at the transmit frequency rather than the natural frequency of each UCA. Therefore, the confocal zone was defined as the time $\pm\ 3T$ from the focus; its physical length ranged from approximately 1.3 to 3.2 mm, depending on the transmit frequency [Fig. 1(b)]. The lengths were designed to always be in the range between the beamwidth of the transmit transducer and depth of focus of the receive transducers (Table I).

Extraneous signals—those containing no bubbles, multiple bubbles, or bubbles out of the confocal zone—were filtered from the data set. Of the 140 000 total acquired signals across all frequencies (40 000 to 50 000 at each frequency), 127 000 were classified and immediately removed

TABLE I. TRANSDUCERS CHARACTERISTICS.

Center frequency	Use	Model	Element diameter [mm]	Focal length [mm]	−3-dB fractional bandwidth	−6-dB beamwidth at focus [mm]	−6-dB depth of focus [mm]	Est. ring-down time const. (τ)
2.8 MHz	Transmit	E9812	19.05	38.3	12.8%	1.27	12.5	$2.5T^*$
4.6 MHz	Transmit	E1066	19.05	37.8	11.1%	0.78	9.2	$2.8T^*$
7.1 MHz	Transmit	E1060	19.05	37.3	15.0%	0.44	5.5	$2.1T^*$
14.6 MHz	Receive	IS1504GP	12.7	27.2	25.6%	0.27	3.6	—
13.8 MHz	Receive	IS1504GP	12.7	27.3	20.9%	0.27	3.8	—

*T is the period associated with the transmit center frequency.

from further analysis; this large rejection rate was due to the total receiving volume being far more likely to contain microbubbles than the smaller confocal region.

After excluding the unambiguous signals that did not contain the response of a single bubble from the confocal region, it was necessary to further classify the remaining signals. The secondary categorization step was designed to mimic prior manual classifications using a peak-detection algorithm to identify local extrema. A peak was explicitly defined as a sample differing from its surrounding samples by at least 0.9ξ, an optimized multiple chosen to match manual classification. To be considered a bubble response, at least one peak was required to exceed the noise threshold in the confocal region, but not all peaks. This method

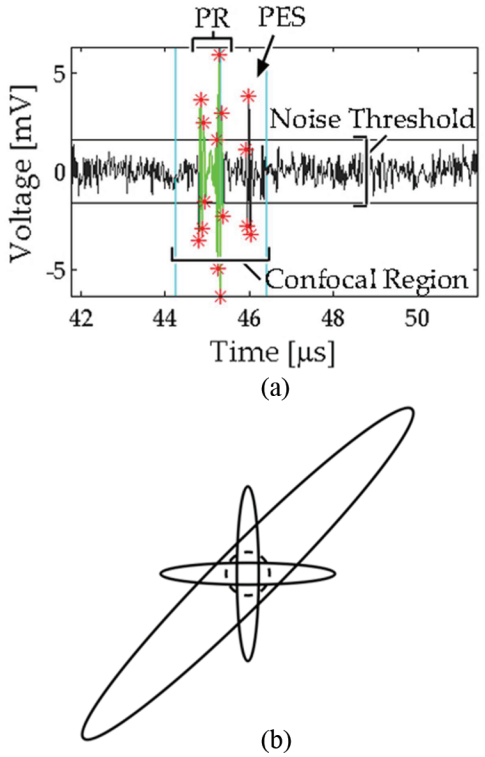

Fig. 1. (a) Single Definity UCA response, insonified at 2.8 MHz and 1.11 to 1.14 MPa PRPA, which contains both a principal response (PR) and a postexcitation signal (PES). The horizontal lines indicate the noise threshold; the vertical lines indicate the confocal zone. Detected peaks are indicated by red stars; the PR is indicated by lighter shading of the RF signal. (b) Cross-sectional illustration of overlapping transmit and receive focal regions (not to scale), with a dotted circle indicating the approximate physical extent of the $\pm 3T$ confocal zone.

of peak definition proved to be more robust with the noisy PCD signals than low-pass-filter- and derivative-based approaches.

Optimized multiples of the period, T, were used to define grouping relationships among the peaks. Closely spaced peaks separated by no more than $1.02T$ were considered to be harmonic and to have originated from a single source. The principal response was defined as the longest sequence of harmonic peaks, and any peaks detected following the end of the PR were considered to be postexcitation peaks. Isolated peaks—those with no other peak detected within $8T$—were considered to be random noise fluctuations and were ignored.

Finally, after identifying the PR and any other peaks, the signal was classified into one of several categories (Table II). If the PR was within the confocal region of both channels and of proper duration, it was considered to come from a single UCA and was categorized based on detection of postexcitation peaks in zero, one, or two channels. Only two cases—PES in both or no channels—were regarded as clearly containing a symmetric, harmonic response for the full duration. Of the 13 000 remaining signals, 1178 fit into these two categories and were statistically analyzed, using Kruskal–Wallis analysis of variance (ANOVA) tests because of the non-normal distribution of residuals. Results were considered significant for a p-value < 0.01.

III. RESULTS AND DISCUSSION

A. Comparison With Manual Classification

To validate the automatic classification, data sets were acquired and manually classified for Definity at 2.8, 4.6, and 7.1 MHz with a range of PRPAs. A least-squares optimization was performed on the three parameters deemed most important for classification: maximum duration of the PR, maximum allowed peak separation within the PR, and algorithmic sensitivity for identifying peaks. The values that minimized the sums of the squared differences compared with manual classification across the full range of PRPAs and transmit center frequencies were selected. These fixed definitions for signal parameters defining peak detection and peak grouping were used across all frequencies and PRPAs to reduce unintentional visual biases from manual classification. The chosen values were still influ-

TABLE II. CHARACTERISTICS OF CLASSIFIED SIGNALS.

Signal classification	Automatic classification definition*
No bubbles	1. No samples in either channel were greater than the noise threshold, ξ.
	2. No closely spaced peaks were identified within the confocal region.
Multiple bubbles	1. The duration of the signal envelope exceeding the noise threshold was greater than 3 times the transmitted pulse duration.
	2a. The PR was greater in duration than the optimized multiple of $4T$.
	2b. Multiple peaks were detected before the PR.
Out of confocal region	1a. The difference in time of arrival, determined through maximizing the cross-correlation between the two channels, exceeded 1 μs.
	1b. The maximum amplitude of the response in either channel exceeded 5 times that in the second channel.
	2a. The PR in either channel occurred outside the confocal region.
	2b. Different classification responses were observed in each channel.
Unknown origin	2. The PR was shorter in duration than $0.5T$.
Single UCA within confocal region	2. The PR was within the confocal region while satisfying minimum and maximum duration requirements. One or more PESs were detected in one, two, or no channels.

*A 1 denotes the process used to eliminate signals in initial step, whereas a 2 indicates steps involving peak detection.

enced by the prior analyses because these new definitions were determined empirically rather than arising out of a theoretical framework; nevertheless, a manually validated and empirically derived algorithm may serve as a starting point for the development of a theoretical framework.

The most comparable fit for the maximum PR duration was $4T$, a value twice as large as the $2T$ that might be expected from an ideal 3-cycle pulse, but one that was suitable when considering the extended transducer ringdown time—perhaps especially in situations in which shell disruption before the end of excitation generated a large free bubble (Table I). For the maximum peak spacing within the PR, $1.02T$ was found to be most similar. This duration was slightly larger than the $1T$ that might be expected of a purely forced harmonic response, but was appropriate when accounting for UCAs that were being insonified at a higher frequency than their natural frequency (i.e., larger UCAs). This duration also established the minimum time for detectability of a postexcitation peak, which was required to be greater than the peak separation value within the PR. Because this detectability varied with frequency (as did the forced PR), the average physical bubble growth and collapse associated with the PES also should be expected to vary with frequency.

Fig. 2 shows the comparison between the automatically and manually classified signals for the three frequencies. Although the agreement was not exact, peak detection captured the same overall trends—namely, that PES percentage increased as PRPA increased, and increased as frequency decreased. The best-fit duration values did vary somewhat with frequency, particularly for 2.8 MHz compared with the two higher transmit frequencies. This suggests that different visual cues were used previously at each frequency, with some disparity in applying the desired guidelines during manual classification. The automatic classifier eliminated this inconsistency by utilizing frequency-independent metrics for signal parameters.

B. Statistics of Postexcitation Rebound

In addition to consistently applied definitions, another advantage of using peak detection and quantitatively defined relationships is that it allows analysis of trends in the principal response and the postexcitation signal. Two questions are of special interest for understanding UCA dynamics: First, is the occurrence of a PES predictable from the PR of the bubble? Second, are there frequency-dependent effects with the PES?

Regarding the first question, previous work has suggested that Definity signals with PES have approximately 4 dB greater broadband noise than those without PES [7], attributed to increased energy in the PR. In this broader study at lower PRPAs and across multiple frequencies, UCAs with PES exhibit greater PR peak amplitude and shorter PR duration (Table III). These results are consistent with the concept of a stronger initial response ultimately leading to postexcitation rebound, perhaps due primarily to initial bubble size and shell properties (resonance-related behavior).

As for the second question, two frequency-dependent effects were noted. First, the mean gap from the end of the PR to the initial PES was clearly linked to the trans-

TABLE III. AVERAGE CHARACTERISTICS OF UCAS WITH AND WITHOUT PES.

	With PES ($N = 844$)	Without PES ($N = 334$)
Amplitude of PR peaks	1.72 (±0.61) × 1.8ξ	1.58* (±0.40) × 1.8ξ
Number of PR peaks	3.99 (±1.43)	3.80 (±1.41)
Duration of PR	2.08 (±0.81) × T	2.32* (±0.78) × T
Ratio of amplitude of PR to PES peaks	1.35 (±0.32)	N/A

*Significant difference from With PES, $p < 0.01$.

TABLE IV. AVERAGE CHARACTERISTICS OF POSTEXCITATION SIGNALS AT THE THREE TESTED FREQUENCIES.

	2.8 MHz ($N = 450$)	4.6 MHz ($N = 298$)	7.1 MHz ($N = 96$)
Initial PES gap (nondimensional)	1.98 ($\pm$1.15) $\times$ T	1.87* ($\pm$1.42) $\times$ T	1.79* ($\pm$1.56) $\times$ T
Initial PES gap (dimensional)	0.71 ($\pm$0.41) μs	0.41* ($\pm$0.31) μs	0.25** ($\pm$0.22) μs
Number of PES rebounds	1.98 ($\pm$1.15)	1.35* ($\pm$0.84)	0.98** ($\pm$0.59)
Amplitude of PES rebounds	1.38 ($\pm$0.38) $\times$ 1.8ξ	1.18* ($\pm$0.18) $\times$ 1.8ξ	1.16* ($\pm$0.16) $\times$ 1.8ξ

*Significant difference from 2.8 MHz, $p < 0.01$.
**Significant difference from 2.8 MHz and 4.6 MHz, $p < 0.01$.

mit frequency, being approximately $2T$ in duration. This means that, in terms of dimensional time, the gap significantly decreased at higher frequencies (Table IV). Second, the average number of postexcitation rebounds following the PR was statistically different across all three frequencies; this value decreased as frequency increased from 2.8 to 4.6 to 7.1 MHz, despite the rebound amplitude only being significantly different at 2.8 MHz. Nevertheless, these two trends correspond with the idea that lower frequency insonification leads to bubbles that persist longer after rupture, because the initial gap was greater and there were more detectable rebounds.

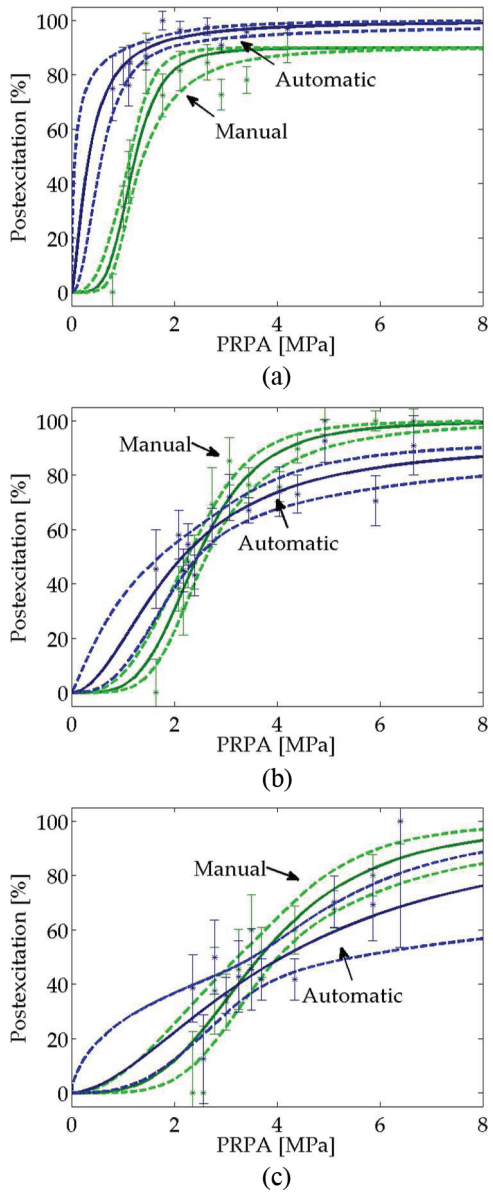

Fig. 2. Comparison between manual classification (green) and automatic classification (blue) of percentage postexcitation curves for Definity UCAs at (a) 2.8 MHz, (b) 4.6 MHz, and (c) 7.1 MHz. The curves indicate a logistic regression fit to the data and the 95% confidence interval.

IV. CONCLUSIONS

An automatic peak-detection classifier was implemented for studying postexcitation rebound of ultrasound contrast agents using double passive cavitation detection. By defining frequency-independent characteristics to group the detected peaks in the time domain, the automatic classifier was able to obtain results similar to visually based manual classification; specifically, there was an increase in the percentage of symmetric single-bubble signals with postexcitation rebound as peak rarefactional pressure increased for a given frequency.

Moreover, quantitative analysis of the detected peaks revealed that there were statistically significant amplitude and duration differences between the principal harmonic responses of UCAs with and without PES, and that both the duration of the gap preceding postexcitation rebound and the number of rebounds depended on the insonifying frequency. These experimental results therefore suggest that insonifying frequency affects symmetric collapse for UCAs by influencing the nature of the generated free daughter bubble or bubbles.

REFERENCES

[1] D. Cosgrove and N. Lassau, "Imaging of perfusion using ultrasound," *Eur. J. Nucl. Med. Mol. Imaging*, vol. 37, suppl. 1, pp. S65–S85, 2010.

[2] N. McDannold, N. Vykhodtseva, and K. Hynynen, "Targeted disruption of the blood–brain barrier with focused ultrasound: Association with cavitation activity," *Phys. Med. Biol.*, vol. 51, no. 4, pp. 793–807, 2006.

[3] M. M. Forbes, R. L. Steinberg, and W. D. O'Brien Jr., "Examination of inertial cavitation of Optison in producing sonoporation of Chinese hamster ovary cells," *Ultrasound Med. Biol.*, vol. 34, no. 12, pp. 2009–2018, 2008.

[4] Y. Birnbaum, H. Luo, T. Nagai, M. C. Fishbein, T. M. Peterson, S. Li, D. Kricsfeld, T. R. Porter, and R. J. Siegel, "Noninvasive in vivo clot dissolution without a thrombolytic drug: Recanalization of thrombosed iliofemoral arteries by transcutaneous ultrasound combined with intravenous infusion of microbubbles," *Circulation*, vol. 97, no. 2, pp. 130–134, 1998.

[5] C. A. Johnson, R. J. Miller, and W. D. O'Brien Jr., "Ultrasound contrast agents affect the angiogenic response," *J. Ultrasound Med.*, vol. 30, no. 7, pp. 933–941, 2011.

[6] D. A. King, M. J. Malloy, A. C. Roberts, A. Haak, C. C. Yoder, and W. D. O'Brien Jr., "Determination of postexcitation thresholds for single ultrasound contrast agent microbubbles using double passive cavitation detection," *J. Acoust. Soc. Am.*, vol. 127, no. 6, pp. 3449–3455, 2010.

[7] M. Santin, D. A. King, J. Foiret, A. Haak, W. D. O'Brien Jr., and S. L. Bridal, "Encapsulated contrast microbubble radial oscillation associated with postexcitation pressure peaks," *J. Acoust. Soc. Am.*, vol. 127, no. 2, pp. 1156–1164, 2010.

[8] D. A. King and W. D. O'Brien Jr., "Comparison between maximum radial expansion of ultrasound contrast agents and experimental postexcitation signal results," *J. Acoust. Soc. Am.*, vol. 129, no. 1, pp. 114–121, 2011.

[9] K. Raum and W. D. O'Brien Jr., "Pulse-echo field distribution measurements technique for high-frequency ultrasound sources," *IEEE Trans. Ultrason. Ferroelectr. Freq. Control*, vol. 44, no. 4, pp. 810–815, 1997.

[10] R. C. Preston, D. R. Bacon, A. J. Livett, and K. Rajendran, "PVDF membrane hydrophone performance properties and their relevance to the measurement of the acoustic output of medical ultrasound equipment," *J. Phys. E*, vol. 16, no. 8, pp. 786–796, 1983.

[11] J. F. Zachary, J. M. Sepsrott, L. A. Frizzell, D. G. Simpson, and W. D. O'Brien Jr., "Superthreshold behavior and threshold estimation of ultrasound-induced lung hemorrhage in adult mice and rats," *IEEE Trans. Ultrason. Ferroelectr. Freq. Control*, vol. 48, no. 2, pp. 581–592, 2001.